Wall fire behavior in an under-ventilated room

Gilles Bertin, Jean-Michel Most*, Mickaël Coutin

Laboratoire de Combustion et de Détonique, Université de Poitiers, UPR 9028 au CNRS-ENSMA, 86961 Futuroscope Chasseneuil Cedex, France

Abstract

An experimental setup has been designed and built to study, at a laboratory scale, the behavior of a wall fire in a semi-confined compartment both in naturally ventilated and vitiated (combustion products) atmospheres.

A diffusion flame is stabilized along a vertical porous flat burner located at the rear of an enclosure. The combustion is supplied by injection of propane through the vertical burner surface. Air enters into the compartment by natural convection through a door, topped by a soffit, opposite the burner. After reaching a thermal steady state, the temperature field in the compartment is characterized. Then, the door is closed leaving only a horizontal free slot (0.06 m height) between the top of the door and the bottom of the soffit. The flame behavior completely changes, the intensity of the spontaneous flame emission decreases drastically and a weakly blue vertical flame leaves the burner surface and moves, at low velocity, through the chamber, up to the open slot. Visualizations of the flame and measurements of the temperature and main stable chemical species fields are performed in order to characterize the behavior of a flame referred as a *ghosting flame*.

This flame displacement mode has been already observed in full-scale fires by Audouin (Fifth International Symposium on Fire Safety Science, 1997, Melbourne, p. 1261–1272). After the initial "flame propagation", combustion can be stabilized at the room aperture that participates to the development of the fire outside the compartment. This work contributes to a better understanding of this phenomenon in order to prevent such a fire. © 2002 Published by Elsevier Science Ltd.

---

*Corresponding author.

E-mail address: most@lcd.ensma.fr (J.-M. Most).

1. Introduction

Many studies have been conducted on the fire behavior in compartment, several reviews were proposed, for example those of Babrauskas et al. [1], Drysdale [2] and Karlsson et al. [3]. They concern mainly the fire growth of small sources, the toxic products and smoke generation, and the characteristic time for a potential transition to flashover. The development of such a room fire is strongly linked to the combustion parameters, the location of the available fuel material, the air mass flow rate feeding the combustion, and the thermal properties of the environment. Moreover, the geometry and the scale of the compartment, and the air supply characteristics can play an important role in the fire growth or size [4], modifying the conditions leading to flashover. Quintiere et al. [5] give similar conclusions as Gross et al. [6] study for a PMMA slab. They show that, on the one hand, for small widths of the opening, the fuel pyrolysis rate increases with the air ventilation as long as mass oxygen fraction is sufficient; and, on the other hand, for larger openings, the mass loss depends on the fuel surface and on the thermal radiation, independently of oxygen excess. These effects of the fire air supply are quantified by Kawagoe [7] through the ventilation factor F_v that takes into account the surface A_0 and the height H_0 of the opening ($F_v = A_0 H_0^{1/2}$). These results underline the great influence of the available air entrainment on the fire characteristics.

During the fire growth period, the air supply can become insufficient to completely feed the flame that leads to an under-ventilated fire. This scenario corresponds to a partial or complete obstruction of the room opening (for example: pipe filter obstruction by smoke particles, containment or control of the ventilation of nuclear plant rooms). Sugawa et al. [8] were the first ones to observe the formation of a blue unsooty flame over a methanol pool fire surface located within a 2 m width, 0.6 m height and 3 m long enclosure. Later, Morehart et al. [9] conducted experiments on flammability limit in confined environment. A lifted flame is observed over the pyrolysis surface and referred as a *ghosting flame*. This flame behavior, similar to the *ghosting flame* obtained by Sugawa's [8], has also been observed by Audouin et al. [10], during a full-scale test. During this last experiment, a liquid hydrocarbon pool fire was ignited on the floor of an enclosure of 3.75 m width, 2.5 m height and 10 m length, with a 0.64 m² opening. A thick smoke is produced and the temperature at the ceiling level reaches 760°C. The overpressure obtained in the room induces the exhaust of the combustion products through the opening, reducing the fresh air entry. Five minutes after ignition, the combustion intensity decreased drastically, the originally yellow flame (soot radiation) turned to blade blue, and a stabilized *ghosting flame* moved to the aperture.

To complete the previous studies developed in our laboratory on the influence of the air entrainment into a wall fire behavior [11–13], the first objective of the present work is to determine the aerothermochemistry conditions leading to an under-ventilated flame. The reduction of the air supply leads to a *ghosting flame* formation moving through the compartment. The second objective is to describe the thermochemical structure of such a flame. A better understanding of these combustion phenomena is essential to develop specific physical models for fire

growth in various confined and vitiated environments in order to predict the flame behavior (extinction or flame persistence).

2. Experimental apparatus

To carry on the research developed at the laboratory on the influence of the containment on a wall fire behavior, our former fire configuration [12] is adopted. The experimental device setup (Fig. 1) consists of an open laboratory scale enclosure with a vertical flat burner opposite the compartment aperture. A buoyant two-dimensional system is then obtained.

2.1. The enclosure

- The enclosure dimensions are 0.62 m in depth, 0.84 m in height and 0.41 m in width, with a soffit (0.19 m height, 0.41 m width) at the top of the aperture (0.65 m × 0.41 m).
- Floor, ceiling and the upper zone of the compartment are covered with refractory fiber material of kerlane type (thickness: 0.05 m, maximum temperature: 1300°C, thermal diffusivity: 10^{-6} m^2/s).
- In the lower part, lateral walls are made in vitroceram windows (a glass supporting temperature up to 800°C) allowing flame visualization. Similar windows are installed on both lateral sides to balance the thermal losses in order to conserve a symmetrical configuration.
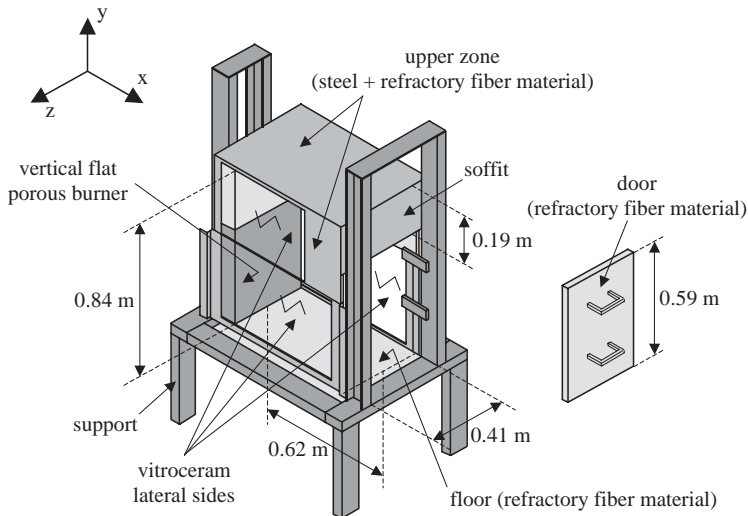

Fig. 1. Experimental apparatus.

- An adiabatic door (kerlane, $0.41\,m \times 0.59\,m \times 0.025\,m$) can be installed at the chamber aperture to reduce the air mass flow rate through a $0.41\,m \times 0.06\,m$ slot between the top of the door and the bottom of the soffit.

2.2. The burner

The fire source is composed of a vertical flat porous burner ($0.40\,m \times 0.50\,m$) located at the rear of the compartment and water-cooled at 65°C. An injection of gaseous hydrocarbon [11–17] through the burner simulates the degradation of a fueled solid material. This operating system dissociates the solid fuel mass flow rate (fire input thermal power) from the heat feedback from the flame. Moreover, the thermal input power is conserved during the test. Industrial propane gas supplies the burner. Only a few complementary tests are performed with pure methane. The hydrocarbon gas mass flow rate is controlled and measured by a mass flowmeter.

3. Diagnostic methods

The used diagnostic techniques are classical and consequently they are not described in this report. The spontaneous flame emission is visualized by a video camera placed in front of the lateral windows in order to follow the flame behavior (shape, color and motion). The thickness of the fresh air inflow, seeded by incense particles, and of the sooted hot combustion products' outward flow are determined by laser tomography (Argon-ion laser sheet). The temperature field in the enclosure is measured with a vertical set of five wire-type K thermocouples (diameter of the
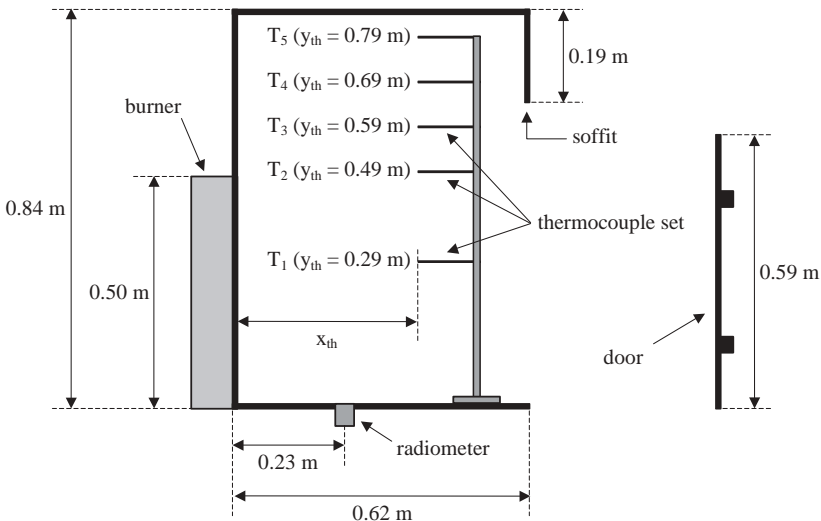

Fig. 2. Location of the measurement probes.

wire and of the cylindrical bead: 200 μm) located in the median plan (Fig. 2). From the compartment floor, the distances y_{th} of the thermocouples T_1, T_2, T_3, T_4 and T_5 are, respectively, 0.29, 0.49, 0.59, 0.69 and 0.79 m. This thermocouple set can be moved in the medium plane ($z_{th} = 0.205$ m) of the enclosure at different distances x_{th} from the burner. The mean volumetric concentration of the chemical species (O_2 and CO_2) is determined at several locations to be discussed later, by isokinetic gas sampling and on-line gas analysis. The radiant heat flux towards the floor from flame, compartment walls and the hot gas layer, is measured by a Medtherm radiometer (view angle: 120°) installed in the floor (Fig. 2), in the median plane of the compartment, 0.23 m from the burner.

4. Test working parameters

Fuel mass rate $\dot{m}_{fuel}$ is the main test parameter, but to compare results obtained with various gases supplied, the theoretical heat release $\dot{Q}$ is considered as the main test parameter ($\dot{Q} = \dot{m}_{fuel} H_c$, where H_c is the heat of combustion of the hydrocarbon). During the experiments, the similarity parameter between real and simulated wall fires is the mass transfer number B [15]. The present B value range is 0.2–0.6, which simulates the degradation of most of the polymers during combustion. The B number is preliminarily determined experimentally from a heat balance at the burner surface [14]. Four $\dot{Q}$ values are selected: 18, 27, 36 and 45 kW (8.5×10^4–2.14×10^5 W/m^3) corresponding, respectively, to propane mass flow rates of 1.88, 2.83, 3.76, 4.71 g/m^2 s (burner surface 0.5 m × 0.4 m) and to B numbers of 0.18, 0.28, 0.37 and 0.46. This $\dot{Q}$ range covers the whole flame behavior: the lower input power corresponds to a flame located essentially along the burner surface, the upper $\dot{Q}$ value leading to a flame whose tip goes out of the compartment. The Grashof number of the system is of order of 10^{11}, so, the flow is strongly driven by buoyancy forces.

5. Main results

The objective of this work is the identification of the combustion behavior when the fire becomes under-ventilated. Consequently, the first part of the study consists of characterizing the thermal properties of the flow when fire is naturally ventilated. The second part of the work describes the behavior and the structure of the *ghosting flame*.

5.1. Characterization of the flame in an open compartment

Fig. 3 shows the flame emission for the two extreme output powers $\dot{Q}$. For $\dot{Q} = 18$ kW, a luminous yellow flame is stabilized along the burner surface. For $\dot{Q} = 45$ kW, the reacting zone emission is more intense. A long and thick flame is deflected by the ceiling, follows down the soffit downward, and leaves the compartment.

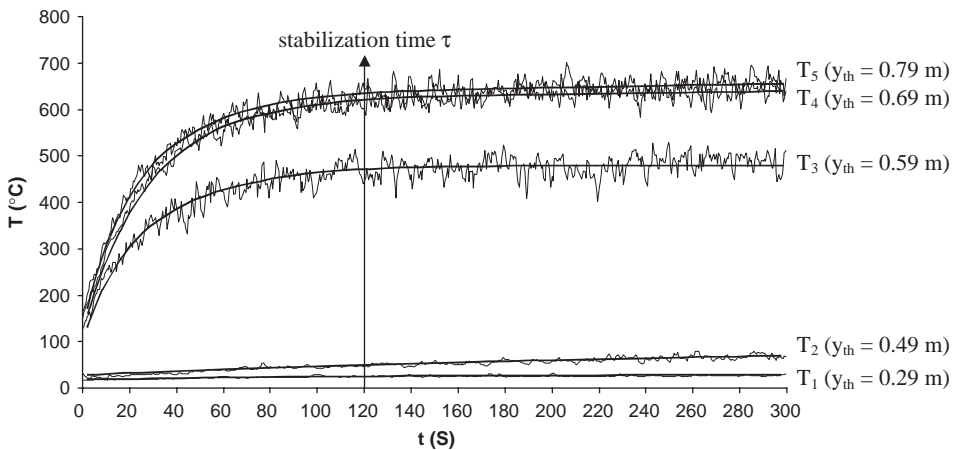Fig. 3. Flame shapes in naturally ventilated atmosphere.

Fig. 4. Typical temperature evolution ($\dot{Q} = 36$ kW, $x_{th} = 0.59$ m, $z_{th} = 0.205$ m).

The thermocouple set is put 3 cm upstream of the aperture ($x_{th} = 0.59$ m) in the symmetrical plane of the compartment ($z_{th} = 0.205$ m). The temperature acquisition starts at the ignition time.

Fig. 4 shows a typical temperature evolution from the flame ignition to the thermal equilibrium in the compartment reached after the delay τ. This stabilization time τ includes the phenomena of water condensation and heat losses in the walls, and then depends on the fixed input thermal power. The τ values obtained for the four considered $\dot{Q}$ values are reported in Table 1.

Fig. 5 represents the vertical variation of the mean temperature for the four considered input powers $\dot{Q}$. These results are also reported in Table 1.

After the thermal equilibrium in the enclosure (time $t > \tau$), the results show flow stratification. A quasi linear increase of the mean temperature maximum in the hot upper zone with $\dot{Q}$ can be deduced from Table 1, as well as a conservation of the hot

Table 1
Thermal characteristics of the compartment after reaching a thermal equilibrium

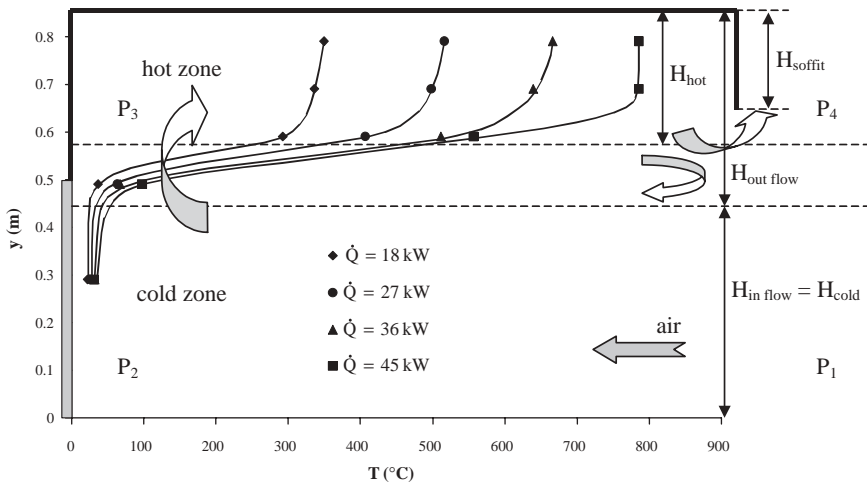| $\dot{Q}$ (kW)	$T_{\text{cold zone}}$ (°C)	$T_{\text{hot zone}}$ (°C)	$\Delta T = T_{\text{hot}} - T_{\text{cold}}$ (°C)	Stabilization time τ (s)	$\dfrac{H_{\text{out flow}} - H_{\text{soffit}}}{H_{\text{in flow}}}$
	$y_{\text{th}} = 0.29$ m $x_{\text{th}} = 0.59$ m	$y_{\text{th}} = 0.79$ m $x_{\text{th}} = 0.59$ m	$x_{\text{th}} = 0.59$ m		
18	22	350	328	240	0.21
27	25	516	491	180	0.28
36	32	666	634	120	0.32
45	31	786	755	90	0.36

Fig. 5. Evolution of the mean temperature after thermal stabilization and for various $\dot{Q}$ values ($x_{\text{th}} = 0.59$ m, $z_{\text{th}} = 0.205$ m).

(H_{hot}) and cold (H_{cold}) layer thickness (Fig. 5). This temperature augmentation of the upper zone is attributed to heat losses through the walls and ceiling, which are functions of the heat release $\dot{Q}$. Temperature measurements are performed in the symmetrical plane of the compartment and for four distances from the burner ($x_{\text{th}} = 0.05$, 0.23, 0.41 and 0.59 m) showing a stratification of the flow. Arrows in Fig. 5 represent the theoretical convective motion observed in such buoyant flows. Moreover, a laser tomography shows an increase of the outward flow thickness with $\dot{Q}$ (last column of Table 1) around a mean value of 30%. These observations are in good agreement with the results reported by Jaluria [18].

These preliminary results qualify our experimental device for a fire behavior study in an enclosure. Later, this equipment can be used for other fire science developments such as flashover studies. The naturally ventilated fire behavior has been observed in the enclosure: flow stratification, smoke layer thickness and thermal characterization of the compartment. The delay τ to reach a steady state thermal

condition was precisely determined in order to assure the same initial conditions at the door closing for studies on the fire behavior in an under-ventilated environment. Moreover, the obtained experimental data for the temperature fields can be easily used to validate numerical results for a fire modeling in an enclosure.

5.2. Wall fire behavior in vitiated atmosphere

When the thermal equilibrium is reached in the enclosure (time $t > \tau$), the aperture is partly closed leaving only a thin horizontal free slot of $0.06 \, \text{m} \times 0.41 \, \text{m}$ between the top of the door and the bottom of the soffit. This small aperture is located in the former hot upper zone (Fig. 5). In these conditions, pressure $P_3 > P_2 > P_1$ and P_3 is higher than P_4, then fresh air cannot enter into the enclosure, the combustion is then completely confined. The fuel injection mass flow rate is kept constant through the burner during the test.

5.2.1. Flame behavior observation

Few seconds after the door closing ($t = 8 \, \text{s}$), the flame decreases rapidly in size and in spontaneous emission intensity (Fig. 6). The yellow radiation from soot becomes imperceptible. A weakly luminous blue vertical plane flame (hydrocarbon radical emission) is observed over which a yellow plume takes place ($t = 13.5 \, \text{s}$). Then, this two-dimensional flame sheet, still presenting a blue and vertical leg topped by a luminous plume, leaves the burner surface and travels in the enclosure at low velocity
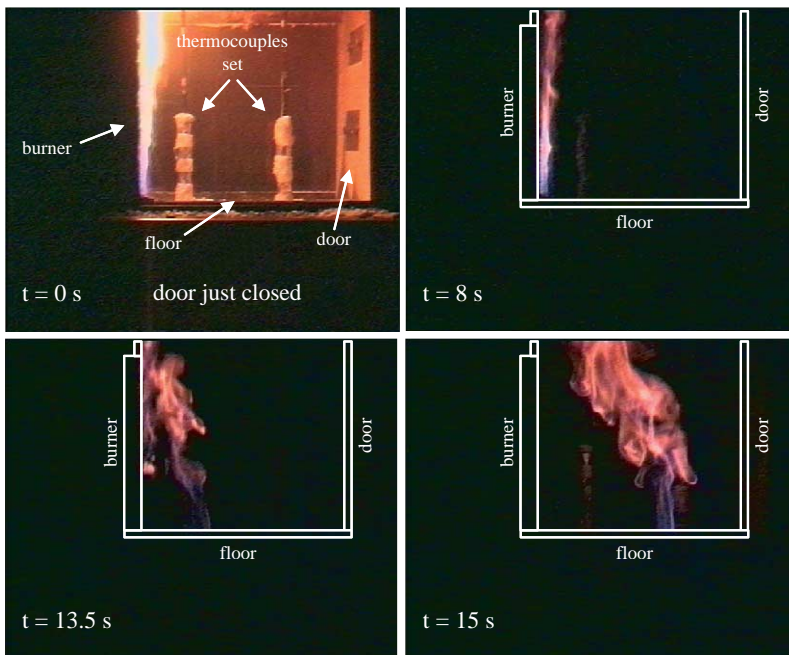

Fig. 6. Ghosting flame visualization.

(few centimeters per second) to the aperture ($t = 15\,\text{s}$). These behaviors seem to look alike those already observed by Sugawa [8] or Audouin [10] where the phenomenon was referred as a *ghosting flame*. Any convective motion seems to affect the flame shape. When the flame reaches the aperture, a re-ignition phenomenon is sometimes observed: fresh air flows quickly into the compartment and ignites the excess of fuel.

This *ghosting flame* phenomenon does not appear or reach the aperture during each test. Sometimes the flame prematurely dies as soon as its "foot" leaves the floor. The results show that the *ghosting flame* observation rate increases with the output power $\dot{Q}$ (statistical study on 20 tests for each $\dot{Q}$ condition, 50% observation for $\dot{Q} = 18\,\text{kW}$, 90% for $\dot{Q} = 45\,\text{kW}$).

5.2.2. Temperature profile through the ghosting flame

The temperature in the enclosure is determined by the thermocouple set during the *ghosting flame* life ($T_1: y_{th} = 0.29\,\text{m}$; $T_2: y_{th} = 0.49\,\text{m}$; $T_3: y_{th} = 0.59\,\text{m}$; $T_4: y_{th} = 0.69\,\text{m}$ and $T_5: y_{th} = 0.79\,\text{m}$). A standard temperature evolution in the room is observed (Fig. 7) when the thermocouple set is located at $x_{th} = 0.41\,\text{m}$ from the rear of the compartment. Each temperature in the whole enclosure increases up to its maximum ($t \approx 11\,\text{s}$ after door closing). During this period, the oxygen is consumed; the heat release by combustion is confined inside the compartment increasing the temperature of each stratified layer. During the next step, the available oxidizer decreases, the thermal losses through the walls become greater than the heat release. At $t = 23\,\text{s}$ the flame passes the thermocouple T_1 ($y_{th} = 0.29\,\text{m}$) which detects an increase of the temperature dT ($T_{max} = 500°\text{C}$, $dT = 260°\text{C}$). This temperature augmentation is also detected by the second thermocouple T_2 ($y_{th} = 0.49\,\text{m}$) but with a smaller amplitude ($dt = 50°\text{C}$). No significant temperature variation is observed
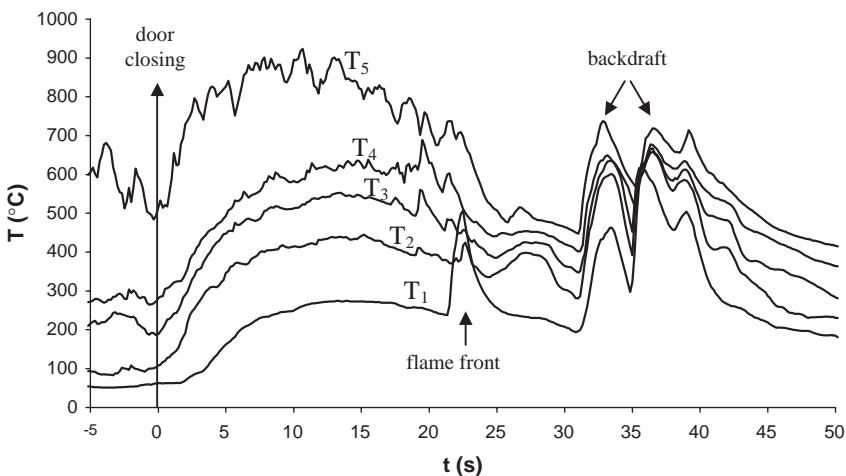

Fig. 7. Temperature evolution during the ghosting flame life ($\dot{Q} = 27\,\text{kW}$, $x_{th} = 0.41\,\text{m}$ and $z_{th} = 0.205\,\text{m}$).

higher. These results show that the blue part of the vertical *ghosting flame* is hotter than its local environment. Higher, the local upper temperature favors soot formation (light yellow plume of flame), the heat release by combustion is not sufficient to induce a temperature increase in the compartment. After the flame passing, the temperature falls back at the quasi-initial level. When the flame reaches the aperture, it generally dies, but sometimes (Fig. 7) a re-ignition of the fuel excess in the enclosure is observed (the fuel gas is still injected through the burner). This last phenomenon can be referenced as *backdraft*.

Similar temperature behaviors are obtained for higher fuel mass flow rates $\dot{m}_{C3H8}$, the temperature and the size of the flame increase (for $\dot{m}_{C3H8} = 0.97$ g/s, equivalent to $\dot{Q}_{th} = 45$ kW, $T_{max} = 800°C$ and dT reaches $500°C$). This result shows that the flame stabilization is mainly related to fuel rather than oxidizer supply.

5.2.3. Chemical composition of the ghosting flame

To complete the *ghosting flame* characterization, volumetric concentrations of the chemical species O_2 and CO_2 are measured. The Y_{O_2} and Y_{CO_2} concentrations are determined in the compartment at $x = 0.31$ m and $z = 0.205$ m for three different locations of the sampling probe over the floor ($y_1 = 0.10$ m, $y_2 = 0.49$ m, $y_3 = 0.69$ m). Three tests are performed with the same working parameters. The time constant of the system (sampling line, analyzer delays) was evaluated to 25 s. It is systematically taken into account to synchronize the gas concentration measurements with the other measurements.

Three main regions can be noticed in Fig. 8. Before the door closing (zone 1), temperature T_1 ($y_{th} = 0.29$ m) and chemical composition Y_i of the fluid correspond to those of a ventilated cavity. The door is closed at time $t = 0$. During the period of zone 2, combustion takes place in the confined environment. The first increase of temperature ($0 < t < 13$ s) is attributed to a heat release in the compartment higher than the heat losses through both the walls (conduction) and the aperture (convection). During this period, the O_2 and CO_2 concentrations are still constant. As soon as the flame leaves the burner surface, O_2 and CO_2 concentration, respectively, decrease and increase ($t > 13$ s). During the flame crossing, any modification of these concentrations is significantly visualized (the time constant of the system can be too large) contrary to the temperature signal (shorter response time). The combustion does not seem to affect the thermal properties of the compartment, except, perhaps for CO concentration (not reported in Fig. 8) that shows a light increase. For $t > 43$ s (zone 3), the temperature continues its decrease, and fresh air enters both increasing the oxygen concentration and diluting the combustion products into the compartment and CO_2.

This concentration evolution is also observed for all other thermal input powers $\dot{Q}$.

5.2.4. Ghosting flame radiation

The flame passing is also detected by a radiometer located on the floor ($x = 0.23$ m). The radiant flux evolution (Fig. 9) presents exactly the same behavior
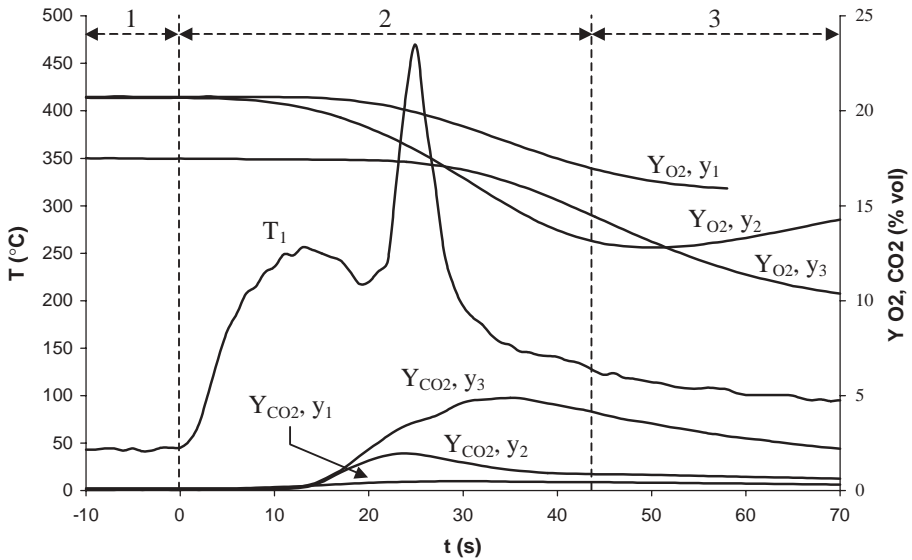
Fig. 8. Temperature, O_2 and CO_2 mean concentration evolutions in the enclosure medium plane ($x = 0.31$ m, $z = 0.205$ m) for $y_{th} = 0.29$ m, $y_1 = 0.10$ m, $y_2 = 0.49$ m and $y_3 = 0.69$ m; and $\dot{Q} = 27$ kW (zone 1: open enclosure, zone 2: confined flame and zone 3: eventual backdraft).
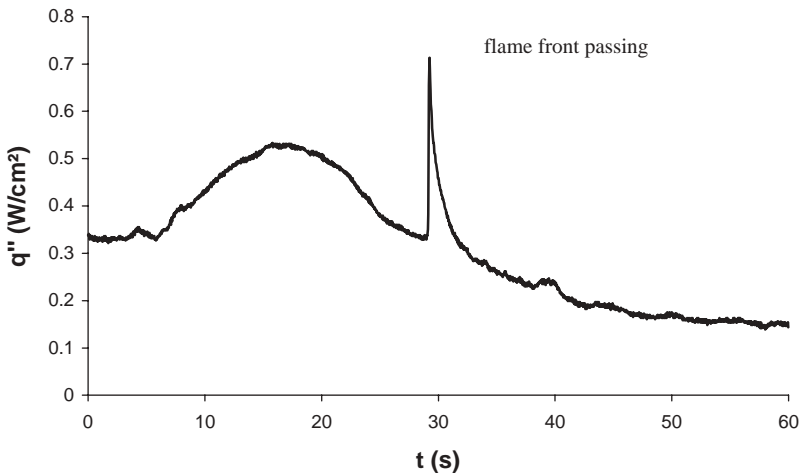

Fig. 9. Evolution of the radiant heat flux to the floor. ($\dot{Q} = 27\,kW$, $x = 0.23$ m, $z = 0.205$ m).

as the temperature signal with a distinct peak of flame radiation when the flame is passing over the radiometer gauge.

5.2.5. Displacement velocity of the ghosting flame

To determine the *ghosting flame* motion velocity, two thermocouples are put respectively at $x_{th\ 1'} = 0.30$ m and $x_{th\ 2'} = 0.33$ m from the burner.
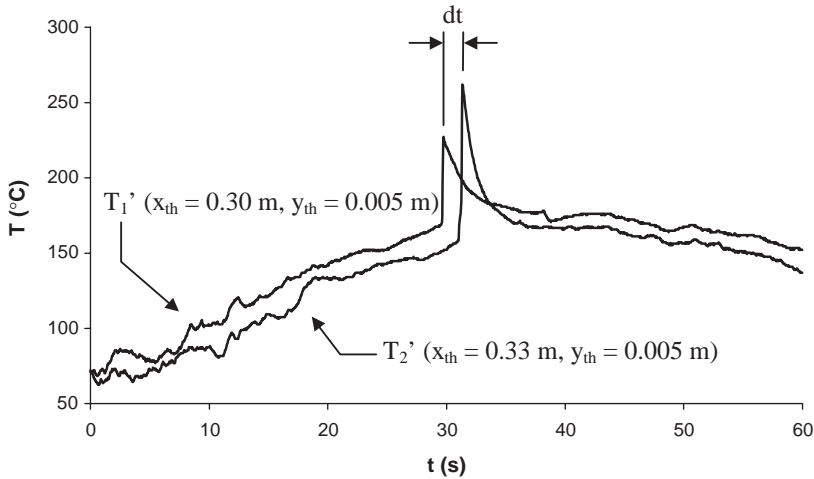
Fig. 10. Temperature variation at the flame passing for ghosting flame motion velocity ($\dot{Q} = 27\,kW$, $x_{th\,1} = 0.30\,m$, $x_{th\,2'} = 0.33\,m$, $y_{th} = 0.005\,m$, $z_{th} = 0.205\,m$).

The velocity of the flame displacement is evaluated by the flight time between thermocouples spacing by 0.03 m. The thermocouples are placed in the medium plane of the enclosure and 0.005 m over the floor. Upstream of the flame front, Fig. 10 shows an evolution with a quasi-linear increase of temperature. At the flame passing, temperature increases by around $T = 250°C$ before coming back to its previous value. The flame transit time between the two thermocouples is then determined. The mean "flame velocity" is deduced and found close to 0.09 m/s, for all injected fuel mass flow rates. This last result is confirmed by image processing of the flame emission during the flame motion in the compartment. This value of the velocity is close to Audouin's results [10] for a *ghosting flame* traveling through a room in a full-scale test.

5.2.6. Hydrocarbon influence: methane

With methane as hydrocarbon, any *ghosting flame* is observed. From the door closing, the stabilized methane flame becomes extremely luminous. Afterwards its luminous intensity and height decrease, and finally the flame vanishes without leaving the porous surface of the burner.

In spite of the absence of the *ghosting flame* phenomenon, the general evolutions of the mean temperature and heat flux in the enclosure are similar to those obtained with propane.

6. Discussion

In this work the confined flame seems to reproduce the phenomena which evolve during the observations to those of the weakly luminous blue flame leaving a pool

fire surface: lifted for Morehart [9], or traveling horizontally to the aperture for Audouin [10]. The structure of this type of combustion is now sought: is a *ghosting flame*, a premixed or a diffusion flame?

The premixed flame structure hypothesis supposes that the flame propagates through a premixing of reactants. The flame moves at 9 cm/s that is close to propane flame velocity at the limit of its flammability [19]. But, this flame structure is not available; the flame does not present the characteristics of preheating, reaction and burnt gases zones.

A diffusion flame structure seems to be more credible. Fig. 11 represents a scheme for the supposed combustion mechanism. The combustion is presumed to be stabilized by a process close to a triple flame one at the floor level where the reactants are premixed before reacting in a blue flame (hydrocarbon radical emission, temperature is still too low ($\approx 500°C$) to induce soot formation). The buoyant forces create an ascendant motion, oxygen and propane diffuse from each side of the reaction zone where the local equivalent ratio is the more favorable for combustion. When the flame reaches the hot zone, the buoyant forces vanish ($\Delta\rho \to 0$), the thermal plume is diluted and soot is produced. Yellow structures, dragged slowly by the blue flame foot, are then observed. Moreover, the flame stays anchored on the floor or dies. This observation is interpreted by a flow downwards of the heavy gas (propane). A small aerodynamic perturbation in the cavity at the floor level induces the blowing and extinction of this unstable flame.

But, why does the flame leave the burner surface and move through the enclosure?

The relaxation of the initial natural convective motion in the buoyant cavity can partly relate this phenomenon simultaneously to combustion effect (reactant mixing) and to the continual gaseous hydrocarbon supply in the enclosure. A simple hydrodynamic model is proposed to evaluate the order of magnitude of the flame motion.
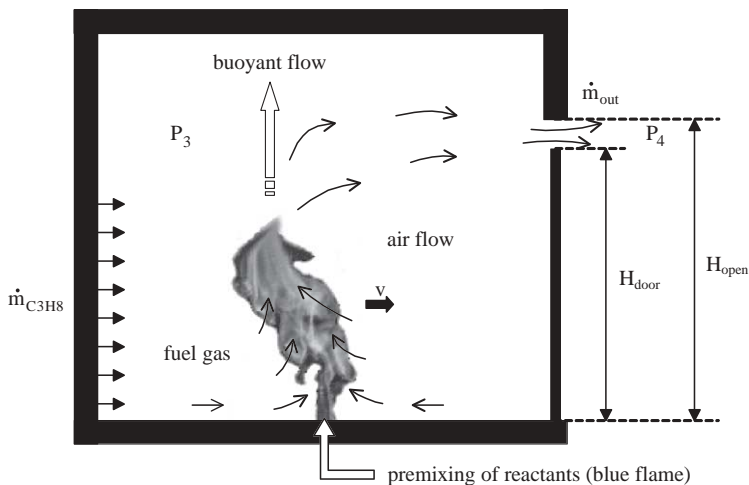

Fig. 11. Ghosting flame mechanism.

6.1. Hydrostatic model

In an open cavity, the density gradient between the cold lower and hot upper zones in the enclosure induces buoyancy driven flow through the opening. When the aperture is partly obstructed, the horizontal thin free slot is located at the previous hot zone level, the density gradient in the enclosure, between H_{open} and H_{door} (Fig. 11) becomes negligible, hence the vertical pressure gradient, is not sufficient to maintain the ventilating motion. The pressure P_3 being greater than P_4, fresh air cannot enter.

From the Bernoulli equation, a calculation of the outward gas mass flow rate $\dot{m}_{out}$ coming out through the free slot is

$$\dot{m}_{out} = \int_{H_{door}}^{H_{open}} l C_d \sqrt{2\rho_{ch}\Delta P_{34}}\, dy,$$

where l is the width of the slot ($l = 0.41$ m), C_d a discharge coefficient (usually $0.6 < C_d < 0.7$ [20]; but for this little slot, a larger value is more credible [3] and $C_d \approx 0.8$), ρ_{ch} is the mean density of the hot gases ($\rho_{ch} = 0.386$ kg/m^3 for $T = 600°C$) and ΔP_{34} is the pressure gradient between the rear of the enclosure and the ambient pressure (Fig. 11).

For a position y located between H_{door} and H_{open}, the P_3 and P_4 pressures are

$$\left. \begin{array}{l} P_3 = P_0 - \rho_{ch}g(y - H_{door}) \\ P_4 = P_0 - \rho_0 g(y - H_{door}) \end{array} \right\} \Rightarrow \Delta P_{34} = P_3 - P_4 = (\rho_0 - \rho_{ch})g(y - H_{door}),$$

where P_0 is the atmospheric pressure, ρ_0 the density of the fresh gas ($\rho_0 = 1.168$ kg/m^3 for $T = 25°C$) and g the gravitational acceleration constant.

Then, the outward gas mass flow rate becomes

$$\dot{m}_{out} = \int_{H_{door}}^{H_{open}} l C_d \sqrt{2(\rho_0 - \rho_{ch})g(y - H_{door})}\, dy$$

$$\Leftrightarrow \dot{m}_{out} = \frac{2}{3} l C_d \rho_{ch} \sqrt{\frac{2g(\rho_0 - \rho_{ch})}{\rho_{ch}}}(H_{open} - H_{door})^{3/2}.$$

A numerical calculation provides a value of $\dot{m}_{out} = 7.82 \times 10^{-3}$ kg/s, leading to a mean output flow velocity of 0.82 m/s at the slot level.

Supposing an homogeneous and steady emptying of hot gases, the mean global flow velocity in the enclosure, corresponding to the mean output flow velocity of 0.82 m/s at the slot level (ratio between slot and compartment section areas), is 0.059 m/s.

The pressure decreases in the enclosure during the steady exhaust inducing a global two-dimensional flow motion, carrying away the *ghosting flame* at the same velocity. Although both continual injection of the gaseous hydrocarbon, combustion effects and species diffusion phenomena are not considered in the hydrostatic model, the obtained results (mean calculated flow velocity: 5.9 cm/s, mean experimental flame velocity: 9 cm/s) are of the same order of magnitude. The relaxation of the

initial natural convective motion and the hot gases enclosure emptying seem to be the principal displacement "engines" of the *ghosting flame* through the enclosure.

In conclusion, a *ghosting flame* seems to be a diffusion flame type, stabilized by a triple flame at the floor level, the combustion products are vertically exhausted by the buoyant forces, the flame motion through the compartment is both assigned to the enclosure emptying and to the combustion effects (species diffusion and triple flame stabilization). This stabilization process is confirmed by complementary tests performed with methane as fuel gas. Methane being lighter than air at the floor, the reactants are not premixed and no *ghosting flame* is observed.

Nevertheless, the modeling of the combustion in an under-ventilated confined compartment remains to be numerically validated and additional measurements are still necessary to better characterize the structure of the flame.

7. Conclusion

During this work, an original device was designed to study a wall fire stabilized inside a compartment both in ventilated and vitiated atmospheres by propane injection through a vertical porous burner. Diagnostic methods were performed to characterize the flame behavior and properties (flame temperature, radiant heat flux to the floor, and gas composition).

In order to get a similar initial condition for all tests, the delay to reach steady state combustion is determined for each burner thermal output power. After closing the door, the containment of the fire leads to transition from a standard ventilated wall fire to a *ghosting flame* traveling through the vitiated compartment up to the aperture.

The *ghosting flame* structure is interpreted as a diffusion flame, anchored at the floor by a triple flame, moving to the aperture with a velocity partially related to the emptying of the compartment. The *ghosting flame* heat release is light with large heat losses on each side of the flame, temperature remaining below $600°C$. At the end of the *ghosting flame* life, a fuel rich region fills the enclosure. The present results confirm Audouin's observations [10] in full-scale experiments. Fuel pyrolysis is sustained by hot wall radiation, the lack of oxygen leads to the formation of a *ghosting flame*. In this last case, the hazard of such a scenario is the formation of a lifted flame stabilized at the room aperture, allowing fire propagation into the building outside the compartment.

References

[1] Babrauskas V, Grayson SJ. Heat release in fires. London: Elsevier, 1992.
[2] Drysdale D. An introduction to fire dynamics, 2nd ed. New York: Wiley, 1999.
[3] Karlsson B, Quintiere JG. Enclosure fire dynamics. Boca Raton, FL: CRC Press, 2000.
[4] Thomas PH. Fires and flashover in rooms—a simplified theory. Fire Saf J, 1980/81;3:67–76.

[5] Quintiere JG, McCaffrey BJ, Den Braven K. Experimental and theoretical analysis of quasi-steady small-scale enclosure fires. 17th Symposium International on Combustion, 1978, Leeds, Angleterre. p. 1125–37.

[6] Gross D, Robertson AF. Experimental fires in enclosures. 10th Symposium International on Combustion, 1964, Cambridge, Angleterre. p. 931–42.

[7] Kawagoe K. Fire behavior in rooms. Building Research Institute, Report No. 27, Ministry of Construction, Tokyo, Japan, 1958.

[8] Sugawa O, Kawagoe K, Oka Y, Ogahara I. Burning behavior in a poorly ventilated compartment fire—ghosting Fire. Fire Sci Technol 1989;9-2:5–14.

[9] Morehart JH, Zukoski EE, Kubota T. Characteristics of large diffusion flames burning in a vitiated atmosphere. Fire safety science. Proceedings of the Third International Symposium, 1992. p. 575–83.

[10] Audouin L, Such JM, Malet JC, Casselman C. A real scenario for a ghosting flame. Fifth International Symposium on Fire Safety Science, Melbourne, 1997. p. 1261–72.

[11] Audouin L. Etude de la structure d'une flamme simulant un incendie de produits industriels. Caractérisation et modélisation de cas réels de feux, Ph.D. thesis. Université de Poitiers, France, 1995.

[12] Coutin M, Most JM, Delichatsios MA, Delichatsios MM. Flame heights in wall fire: effects of width, confinement and pyrolysis length. Sixth International Symposium on Fire Safety Science, Poitiers, 1999.

[13] Coutin M. Etude expérimentale et théorique de l'influence de l'entraînement naturel de l'air sur le comportement d'une flamme représentative d'un incendie, Ph.D. thesis. Université de Poitiers, France, 2000.

[14] De Ris J. The role of buoyancy direction, radiation in turbulent diffusion flames on surfaces. 15th Symposium International on Combustion, 1975. p. 175–82.

[15] Most JM, Sztal B, Delichatsios MA. Turbulent wall fires: LDV and temperature measurement and implications. Proceedings of the Second International Symposium on Applications of Laser Anemometry to Fluid Mechanics, Lisboa, Portugal, 1984.

[16] Annarumma M, Audouin L, Most JM, Joulain P. Velocity and measurements in a bidimensional pool fire: influence of a vertical wall close to the fire. Proceedings of the 12th ICDERS, Dynamics of Deflagrations and Reactor Systems: Heterogeneous Combustion, vol. 132. Prog. Astronaut. Aeronaut., 1991. p. 314–38.

[17] Annarumma M, Audouin L, Most JM, Joulain P. Wall fire close to an horizontal surface: numerical modeling and experimental validation. Fire Mater 1992;16:1–13.

[18] Jaluria Y. Natural convection wall flows, the SFPE handbook of fire protection engineering, 1st ed. Boston, MA, USA: Society of Fire Protection Engineering, 1988 (Chapter 1–7).

[19] Lewis B, von Elbe G. Combustion, flames and explosions of gases, 3rd ed,. Orlando, FL: Academic Press, 1987.

[20] Rockett JA. Fire induced gas flow in an enclosure. Combust Sci Technol 1976;12:165–75.